

RESEARCH ARTICLE

Hemolymph supply to locomotor muscles of the ghost crab *Ocypode quadrata*

Siyuan Yang, Tera D. Douglas, Ryan Ruia and Scott Medler^{*‡}**ABSTRACT**

Ghost crabs are the fastest and most aerobically fit of the land crabs. The exceptional locomotory capacity of these invertebrate athletes seemingly depends upon effective coupling between the cardiovascular system and skeletal muscles, but how these systems are integrated has not been well defined. In the present study, we investigated the relationship between aerobic muscle fibers within the skeletal muscles used to power running and the blood vessels supplying these muscles. We used histochemical staining techniques to identify aerobic versus glycolytic fibers and to characterize membrane invaginations within the aerobic fibers. We also determined how the diameters of these two fiber types scale as a function of body size, across two orders of magnitude. Vascular casts were made of the blood vessels perfusing these muscles, and special attention was given to small, capillary-like vessels supplying the fibers. Finally, we injected fluorescent microspheres into the hearts of living crabs and tracked their deposition into different muscle regions to quantify relative hemolymph flow to metabolic fiber types. Collectively, these analyses demonstrate that ghost crab muscles are endowed with an extensive arterial hemolymph supply. Moreover, the hemolymph flow to aerobic fibers is significantly greater than to glycolytic fibers within the same muscles. Aerobic fibers are increasingly subdivided by membrane invaginations as crabs increase in size, keeping the diffusive distances relatively constant. These findings support a functional coupling between a well-developed circulatory system and metabolically active muscle fibers in these invertebrates.

KEY WORDS: Skeletal muscles, Ghost crabs, Arterial system, Aerobic muscle fibers

INTRODUCTION

Ghost crabs are highly active terrestrial crustaceans specialized for fast running. The genus name, *Ocypode* ('swift-footed'), provides an apt description of these crabs that can attain speeds of 3–4 m s⁻¹ when running at full speed (Hafemann and Hubbard, 1969; Herreid and Full, 1988). In addition to short sprints, ghost crabs are capable of sustaining a prolonged, slow walking gait for 40 min or more (Full and Herreid, 1983; Herreid and Full, 1988). Upon the transition from rest to submaximal running, O₂ consumption increases to steady state within 2 min and is maintained throughout exercise (Full and Herreid, 1983; Herreid and Full, 1988). The aerobic scope for ghost crabs is up

12-fold, which puts them on par with mammals and insects in their ability to elevate O₂ consumption during exercise (Herreid and Full, 1988). Compared with other land crabs, ghost crabs are exceptional in both their running speed and endurance (Herreid and Full, 1988). Fiddler crabs share membership in the family Ocypodidae, but ghost crabs exhibit an aerobic capacity three times greater than these closest relatives (Herreid and Full, 1988). Other terrestrial and semi-terrestrial crabs depend more upon mixed glycolytic/aerobic or purely glycolytic metabolic processes to power locomotion (Herreid and Full, 1988).

The aerobic exercise performance of these invertebrate athletes suggests specialized mechanisms within the cardiovascular system and skeletal muscles to deliver O₂ and generate ATP, but very little is known about the physiological adaptations that support sustained muscle power output. Many decapod crustaceans exhibit a distinct anatomical and physiological division between dark, aerobic muscle fibers and light, glycolytic fibers in different regions of the same muscles (Medler and Mykles, 2015). Specialized swimming muscles in blue crabs and other members of the Portunidae exhibit physiological adaptations that facilitate sustained, aerobic power output (Hardy et al., 2006, 2009, 2010; Henry et al., 2001; Hoyle, 1973; Hoyle and Burrows, 1973; Johnson et al., 2004; Tse et al., 1983; White and Spirito, 1973). These swimming muscles include dark fibers that are effectively subdivided by membrane invaginations lined with high densities of mitochondria. As fiber diameters become larger with growth, the subdivisions expand to keep the effective diameter nearly constant (Hardy et al., 2006, 2009, 2010; Johnson et al., 2004). These membrane invaginations are understood to help overcome diffusional limitations in O₂ delivery to the mitochondria within the muscles (Kinsey et al., 2007). In a previous study, we reported similar mitochondrial-lined invaginations within the populations of aerobic fibers of ghost crab skeletal muscles (Perry et al., 2009). It appears that these mitochondria-packed invaginations are a design feature typical of many crustacean aerobic muscle fibers (Medler and Mykles, 2015). One goal of the present study was to better understand the organization of the aerobic fibers in these terrestrial runners.

Highly aerobic vertebrate skeletal muscles have been studied intensively, and several common patterns are clear. The aerobic capacity of whole animals is strongly correlated with the mitochondrial volume within skeletal muscles (Weibel and Hoppeler, 2005). Mitochondrial volumes in some especially aerobic vertebrate muscles occupy between 21 and 68% of the total fiber volume (Moon and Tullis, 2006). Mitochondrial fractional volumes are typically paired with proportional capillary densities for effective O₂ delivery (Mathieu-Costello, 1993; Weibel and Hoppeler, 2005). Highly aerobic muscles are also typically composed of small diameter fibers, which is another important adaptation to increase capillary density and overcome diffusional limitations (Mathieu-Costello, 1993). Sustained aerobic exercise may elicit adaptive growth in the density of capillaries in active skeletal muscles (Brodal et al., 1977;

Biology Department, SUNY Fredonia, Fredonia, NY 14063, USA.

*Present address: Physician Assistant Studies, St Bonaventure University, St. Bonaventure, NY 14778, USA

‡Author for correspondence (smedler@sbu.edu)

 S.M., 0000-0002-7778-0928

Glaser et al., 2010; Saltin and Gollnick, 1983; Waters et al., 2004). Mice selected over multiple generations for voluntary running behavior exhibit significantly greater capillary densities in their skeletal muscles than controls (Wong et al., 2009).

By comparison, very little is understood about the relationship between hemolymph supply and skeletal muscle organization in invertebrates. Decapod crustaceans are of particular interest in this area, because they possess a circulatory system that seems to be almost intermediate between an open and a closed system (McGaw, 2005; Reiber and McGaw, 2009). The terms ‘hemolymph’ and ‘blood’ are often used interchangeably in the crustacean literature, but we will use the term hemolymph, because the fluid ultimately leaves the blood vessels to bathe the tissues. Well-developed arteries leave the heart to supply all bodily systems in these animals. Within the tissues, blood vessels branch multiple times until they form small capillary-like vessels that supply the tissues. However, the terminal ends of these capillaries empty into open hemolymph sinuses, rather than connecting with small venules. The hemolymph from the sinuses ultimately makes its way back to the heart and re-enters the heart through multiple ostia (Hill et al., 2016; McGaw and Reiber, 2015; McMahan and Burggren, 1988). Many decapod crustaceans are highly alert and active animals that depend upon the efficient supply of hemolymph to sustain these activities.

In the present study, we focused on defining the relationships between cardiovascular hemolymph supply and skeletal muscle in the Atlantic ghost crab, *Ocypode quadrata*. Two of the major skeletal muscles powering locomotion in these crabs are the extensor and flexor of the carpopodite (Burrows and Hoyle, 1973; Perry et al., 2009; Whittemore et al., 2015). We hypothesized that the hemolymph supply to these muscles is well developed to support the metabolic demands of their extraordinary running capabilities. Moreover, we were interested in whether the well-developed aerobic fibers of ghost crabs received a more extensive hemolymph supply than the much larger, anaerobic fibers. We used complementary methods to assess the links between muscle fiber aerobic capacity and hemolymph supply. First, we used histochemical staining techniques to identify aerobic muscle fibers and their structural features, including mitochondrial densities and membrane invaginations. Second, we made vascular casts to reveal the organization of the blood vessels that supply the muscles within the meropodite. Finally, we injected fluorescent microspheres into the hearts of live crabs and tracked their deposition into different muscle regions. Retrieval and quantification of these microspheres permitted us to compare the relative hemolymph flow into different muscle regions.

MATERIALS AND METHODS

Animals

Atlantic ghost crabs [*Ocypode quadrata* (Fabricius 1787)] were supplied by Gulf Specimen Marine Laboratories, Inc. (Panacea, FL, USA) and were also collected from beaches near Nagshead, NC, USA. Live crabs were transported to the State University of New York at Fredonia campus and maintained in aquaria with circulating artificial seawater at 25°C. Crabs were fed dried krill and other commercially available foods formulated for land crabs (Tetrafauna Hermit Crab Cakes, Spectrum Brands Pet LLC, Blacksburg, VA, USA) on a daily basis. In addition, live crickets were periodically fed to the crabs to supplement their staple diet.

Skeletal muscle histochemistry

Skeletal muscle anatomy and metabolic condition (aerobic versus glycolytic) were assessed as previously described in Perry et al.

(2009). Briefly, whole crabs were frozen by rapid immersion in liquid N₂ and tissues were stored at –80°C until used for analyses. To prepare muscle sections, individual legs were isolated from the rest of the body. The second and third walking legs were used in the present study, because these appendages are the primary ones used to power locomotion (Burrows and Hoyle, 1973; Whittemore et al., 2015). The meropodite was divided into proximal, mid-region and distal sections and mounted on aluminium chucks for sectioning with a Leica cryostat. Frozen muscles were placed inside the cryostat chamber and allowed to warm to –20°C. Muscle cross-sections (15 µm) were cut and placed onto coated microscope slides (Fisherbrand Superfrost slides, Thermo Fisher Scientific, Waltham, MA, USA). Tissue sections on slides were then stored at –20°C until the time they were used for histochemistry.

Muscle sections were labeled for aerobic capacity using NADH tetrazolium reductase following the methods described in Dubowitz and Sewry (2007). Briefly, a working solution of nitro-blue tetrazolium (NBT; 0.8 mg ml⁻¹) and NADH (0.64 mg ml⁻¹) was freshly prepared in 50 mmol l⁻¹ sodium phosphate buffer pH 7.4. Muscle tissue sections were permitted to air dry at room temperature for 30 min and were then covered with the NBT/NADH solution. Sections were left to incubate in the dark for 30 min. Sections were then rinsed thoroughly in deionized water and dehydrated through a graded ethanol series. Finally, the sections were cleared with two xylene rinses and mounted with Permount (Thermo Fisher Scientific). This procedure labels aerobic tissues as dark blue or purple, while glycolytic fibers remain light in coloration.

Muscle fiber dimensions

Diameters of aerobic and glycolytic fibers were determined for crabs ranging in size from approximately 1.5 to 100 g. Measurements were made from printed micrographs using electronic calipers to the nearest 0.01 mm (~0.1 µm at the final printed magnification). We applied the ‘lesser diameter’ method described by Dubowitz and Sewry (2007) to determine fiber diameters. The diameter is defined as the maximum diameter across the lesser aspect of the muscle fiber and is designed to overcome the distortions that occur when fibers are sectioned at an oblique angle. We measured at least 20 fibers of each type, from each of the individual crabs. The values presented are the means of those fibers.

Blood vessel anatomy

Blood vessels supplying the leg muscles were revealed using Batson polymer as described by McGaw and Reiber (2002), with minor modifications. We used a Batson’s No. 17 plastic replica and corrosion kit (catalog no. 07349, Polysciences, Inc., Warrington, PA, USA). Batson’s resin corrosion is a partially polymerized monomer which fully polymerizes into durable plastic after it is mixed with a catalyst and promoter. We diluted the polymer by mixing it with methacrylate acid methyl ester at a ratio of 4:1 (methacrylate: polymer) and a red pigment was added to this mixture for visualizing and contrasting the capillaries from surrounding muscles. The monomer solution was then mixed with promoter and catalyst per manufacturer’s instructions and the solution was injected into the cut artery at the proximal end of the meropodite. After successful injection into a blood vessel, the preparation was left to polymerize for at least 30 min.

Complementary analyses were employed to ascertain the overall morphology of the main artery and its branches within the meropodite. The proximal, cut end of the artery was identified by adding a small amount of Methylene Blue dye near the artery and permitting it to stain for 5–10 min. Next, the preparation was rinsed

and the trunk of the vessel could be visualized from the blue staining. The vessel was then grasped with fine forceps and gently pulled toward the distal end of the meropodite. The vessels did not seem to be firmly attached to the muscles and were pulled free from the muscles with little resistance. The entire vessel was then placed into a large drop of Methylene Blue dye and allowed to stain for 5–10 min. Then stained vessels were placed into crab Ringer's solution (458 mmol l⁻¹ NaCl, 8 mmol l⁻¹ KCl, 2 mmol l⁻¹ MgCl₂, 8 mmol l⁻¹ NaHCO₃, 20 mmol l⁻¹ CaCl₂, pH 7.0) (Burrows and Hoyle, 1973) and studied through a stereomicroscope. Vessels were preserved by air drying flat on a microscope slide. The dried vessels were then dehydrated through a graded ethanol series and cleared through two washes in xylenes. The vessels were then permanently mounted in Permount under coverslips. We also attempted to stain any organized f-actin filaments within excised blood vessels using a fluorescently labeled phalloidin (Alexa Fluor 488 Phalloidin, Thermo Fisher Scientific). Vessels were air dried onto microscope slides before incubating for 30 min with the phalloidin probe. Small pieces of cardiac muscle from crabs were used as a positive control. Labeled tissues were observed with a Leica stereomicroscope (model MSV269) fitted with a filter set that provided an excitation wavelength of 490 nm and an emission wavelength of 525 nm (Chroma 49002; Chroma Technology Corp, Bellows Falls, VT, USA).

Microsphere hemolymph flow analyses

To track hemolymph flow into muscle tissues in live crabs, 3.7 μm diameter red fluorescent microspheres (FluoSpheres catalog no. F8858, Thermo Fisher Scientific) were injected into the hearts of five large crabs (mean body mass 43.4±13.7 g). These ~4 μm microspheres were selected because they closely approximate the dimensions of capillaries, whereas larger microspheres (~15 μm) became lodged in vessels upstream of the capillary-like vessels. A volume of 50 μl of the microsphere solution (~3.6×10⁷ microspheres) was mixed well with 450 μl crab Ringer's solution and drawn into a 1 ml syringe fitted with a 29 gauge hypodermic needle. Prior to injection, each crab was placed on an ice water slurry to sedate and immobilize the animal. The microsphere suspension was then injected slowly with constant pressure through carapace into the heart over a period of approximately 1 min. After injection, each crab was placed on a warm wet towel to help warm up so that the pumping heart could distribute the microspheres to active muscles. The crabs were positioned in sunlight in the laboratory and permitted to regain normal activity for approximately 1 h. Crabs were then flash frozen by immersion in liquid N₂ and stored at -80°C until individual legs could be removed and their muscles examined.

Fluorescent microspheres were visualized using a Leica stereomicroscope (model MSV269) fitted with a filter set that provided an excitation wavelength of 560 nm and an emission wavelength of 630 nm (Chroma 49008; Chroma Technology). The second or third walking legs were removed from crabs and viewed under fluorescent illumination. Microspheres were visible through the exoskeleton and appeared to be especially concentrated in the most proximal and distal regions of the muscles. The exoskeleton and underlying integument were then removed from the legs, so that the skeletal muscles could be viewed directly.

Following the visual inspection of microspheres deposited in intact muscles, the muscle tissues were collected from specific anatomical regions (proximal, mid-region and distal) and injected microspheres were recovered from the isolated tissues, using the methods described by Gerry and Ellerby (2014). Briefly, a muscle

digestion was set up by mixing muscle tissue with 1 mol l⁻¹ KOH at a ratio of approximately 15:1 (KOH:muscle volume). Next, the tubes were placed in a water bath at 60°C for 24 h, and then centrifuged at 1500 g for 15 min to spin the pellets down. After centrifugation, the supernatant was pipetted out from the tubes, and the insides of tubes were washed with MilliQ H₂O 0.01% (Tween 20) detergent to ensure that the fluorescent beads would not stick to each other. After being washed, the tubes of microsphere samples were vortexed well in order to ensure that they did not clump. Samples of the microsphere suspensions (10 μl) were loaded onto a standard hemocytometer and viewed using the fluorescence microscope. Known dilution factors were used to determine the original number of microspheres per milligram of fresh muscle tissue.

Statistical analyses

Muscle fiber diameters (μm) were plotted as a function of crab body mass (g) and a logarithmic regression line was fitted to the data. The mean number of fluorescent microspheres deposited in different muscle regions (proximal, mid-region, distal) were compared using an ANOVA model with a block design. Briefly, the ANOVA model included two factors (muscle region and animal), where the specific animal from which measurements were taken served as a block parameter to account for variability and increase the power of the analysis (Neter et al., 1990). A Tukey's *post hoc* ANOVA test was used to compare individual means of microspheres collected from the three muscle regions. Statistical analyses were performed using JMP software version 10.0.2 (SAS Institute, Cary, NC, USA).

RESULTS

General muscle organization

The meropodite is filled with skeletal muscles organized to flex and extend the carpopodite during walking and running. The specific organization of the flexor and extensor of the carpopodite have been described previously (Perry et al., 2009; Whittemore et al., 2015), but additional details are presented here. The two muscles are oriented parallel to one another, with the extensor being in the more anterior position (Fig. 1). In muscle cross-section, it was difficult to discern the separation between the two muscles (Fig. 1B). However, the extensor apodeme lies in a more superior position than the flexor apodeme (Fig. 1B), which provided an anatomical cue to distinguish the muscles. Both muscles possess anatomical clusters of aerobic fibers in the proximal and distal regions (Fig. 1) (Perry et al., 2009). The bulk of the fibers in each muscle is composed of large, white glycolytic fibers with few mitochondria. The blood vessel supplying the muscles was sandwiched between the extensor and flexor (Fig. 1B).

Muscle fiber type characteristics

Glycolytic fibers were larger in diameter than aerobic fibers (Figs 1–3) in all sizes of crabs studied. Aerobic fibers displayed even margins in smaller crabs but possessed conspicuous membrane invaginations in larger crabs (Fig. 2). As crabs grew, the aerobic fibers were progressively subdivided by membrane clefts, so that the effective fiber diameter stayed relatively constant, reaching an asymptote at approximately 70–80 μm (Fig. 3). The fiber subdivisions first became apparent in crabs of approximately 20 g and became more obvious in the muscles from larger crabs.

Blood vessels supplying the leg musculature

The sternal artery in decapod crustaceans leaves the ventral surface of the heart and eventually branches into the arteries supplying each leg.

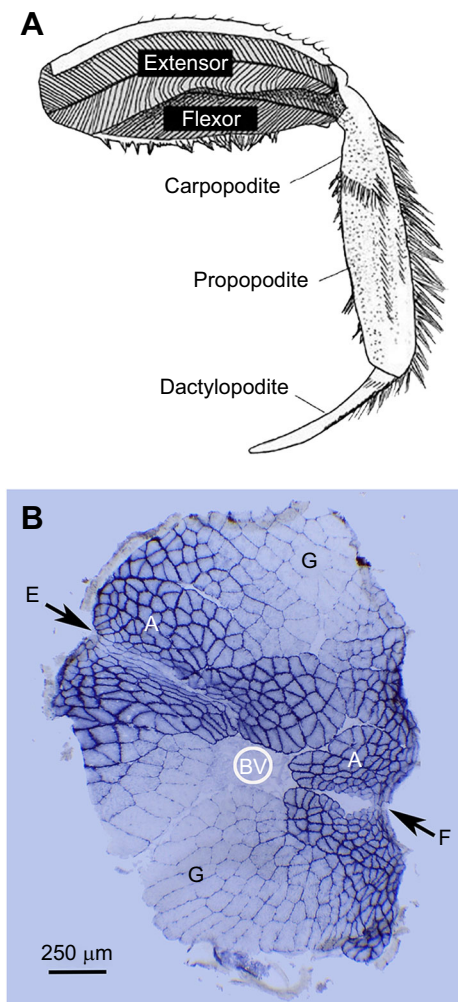


Fig. 1. Organization of extensor and flexor of the carpopodite in the ghost crab *Ocypode quadrata*. (A) The extensor and flexor muscles lie in parallel, with the extensor being anterior to the flexor. These two muscles are enclosed within the meropodite of each of the eight walking legs (modified with permission from Perry et al., 2009, fig. 1A). (B) Cross-section of extensor and flexor muscles. Muscle section was stained for mitochondrial enzymes using NADH-tetrazolium reductase (deep blue staining). The locations of the extensor (E) and flexor (F) apodemes are indicated by the arrows. Staining patterns reveal highest mitochondrial densities near the sarcolemma. Aerobic fibers (A) are regionally distinct from the more glycolytic (G) fibers. The main blood vessel (BV) is enclosed between the extensor and flexor muscles. This section is from the proximal region of the walking leg of a small (1.6 g) crab.

These brachial arteries course between the extensor and flexor muscles within the meropodite and continue all the way to dactyl (Figs 1B and 4). Secondary branches emerged at regular intervals from the main artery and carry hemolymph into the dorsal and ventral muscle regions (Fig. 4A,B). These vessels continued to branch into tertiary branches, creating an extensive hemolymph supply to the muscles. The terminal capillary-like vessels were approximately 1–2 μm in diameter and exhibited extensive branching to the muscle fibers (Fig. 4C,D). Microscopic observations of the larger vessels were consistent with the standard understanding that the blood vessels are composed of collagen-containing connective tissues without any obvious muscular component. The terminal ends of vessels, including the capillary-like vessels, appeared to consist of a single squamous layer of cells. All attempts to identify organized muscle fibers or myofibrils within the artery using fluorescent phalloidin

were negative, whereas the striated cardiac muscle fibers stained strongly (data not shown).

Microsphere deposition in different muscle regions

Examination of leg muscles following microsphere injection revealed that these $\sim 4 \mu\text{m}$ spheres were deposited throughout the extensor and flexor muscles. Using the stereomicroscope equipped with fluorescence illumination, we were able to detect a red glow of the microspheres through the intact exoskeleton (data not shown). Removal of the exoskeleton and underlying integument provided a clear view of the deposition patterns within the muscles (Fig. 5C). Microspheres appeared to be deposited throughout the muscles but were visibly more concentrated in the more aerobic fibers within the proximal and distal regions of the muscles (Fig. 5C).

In a few instances, cold-anesthetized crabs were studied under the stereomicroscope and we were able to visualize fluorescent microspheres through the exoskeleton and observe some of their movements. While most of the microspheres were lodged among the muscle fibers, a few could be observed moving freely within the hemolymph of the legs and flowing in streams back toward the body. Although we did not attempt to formally study these patterns of movement, the principal location appeared to be along ridges of exoskeleton near the dorsal or ventral margins of the meropodite.

Following muscle tissue digestion with KOH, the numbers of microspheres from different regions of the muscles (proximal, mid-region and distal) were determined (Fig. 6). A significant effect of the specific crab was found from the ANOVA ($F=8.26$, $P<0.0061$), indicating that application of ‘crab’ as a block in the model was appropriate to increase the statistical power. A significant effect of muscle region was also recorded ($F=46.20$, $P<0.0001$). A Tukey’s *post hoc* ANOVA test showed that the mid-region fibers had significantly fewer microspheres deposited around them than either the proximal or distal fibers (Fig. 6).

DISCUSSION

The major finding of the present study is that ghost crabs possess a highly developed vascular system, well organized to supply hemolymph to major muscles used to power locomotion. The aerobic fibers within the flexor and extensor muscles receive a larger proportion of the hemolymph compared with glycolytic fibers within the same muscles, as tracked with microsphere injections (Figs 5 and 6). This method of tracking microspheres has been used to estimate blood flow into skeletal muscles and has served as a proxy for metabolic energy usage by these muscles (Gerry and Ellerby, 2014; Marsh and Ellerby, 2006; Marsh et al., 2004). Hardy et al. (2009) injected small fluorescent microspheres (0.2 μm) into the cardiovascular system of blue crabs and then traced the hemolymph flow into the muscles specialized for power swimming. Consistent with our findings, they demonstrated that the aerobic fibers receive more hemolymph than glycolytic fibers and that membrane clefts of aerobic fibers are well perfused by hemolymph (Hardy et al., 2009). Similar patterns have been documented in leg muscles of spiders, where greater amounts of hemolymph were observed around histochemically identified aerobic fibers, as compared with anaerobic fibers within the same muscles (Paul et al., 1994). The selective coupling between the cardiovascular system and the aerobic skeletal muscles provides a better mechanistic understanding of the remarkable aerobic capacity of ghost crabs. Ghost crabs exhibit an aerobic scope of approximately 12-fold, which puts them on par with mammals and reptiles and is several times greater than that of other land crabs (Herreid and Full, 1988).

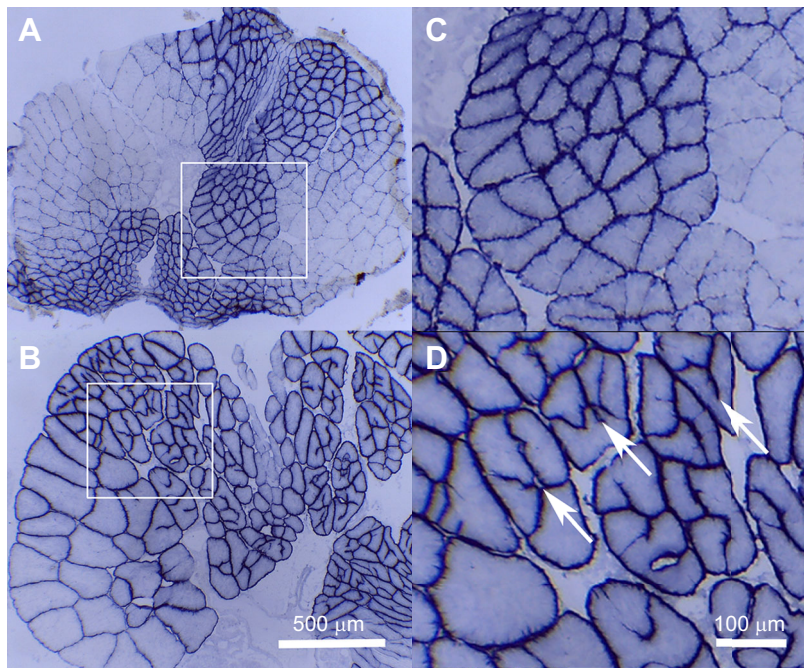


Fig. 2. Aerobic fiber morphology in small (1.6 g) versus large (63 g) *O. quadrata* crab muscles. Muscles were stained with NADH-tetrazolium reductase as in Fig. 1B. (A,B) Lower magnification images show light-staining glycolytic fibers and deep-staining aerobic fibers in small (A) and large (B) crabs. (C,D) Higher magnification images correspond to the highlighted regions in A and B, respectively. The aerobic fibers from the large crab exhibit membrane clefts (arrows in D) that effectively subdivide these fibers into partitions with diameters similar to the undivided aerobic fibers in the smaller crab. However, the light-staining glycolytic fibers are much larger in the 63 g crab than in the 1.6 g crab.

Crustacean muscles typically display a significant degree of functional specialization and exhibit clear diversity among fiber types (Hoyle, 1983; Medler and Mykles, 2015). Specialized fiber types are defined by specific assemblages of alternate isoforms of myofibrillar proteins and by a range of sarcomere widths (Medler and Mykles, 2015). The glycolytic and aerobic fibers differ in the myofibrillar isoforms they express and exhibit unique structural features (Perry et al., 2009). For example, the myofibrils within glycolytic fibers possess shorter sarcomeres ($\sim 3.5 \mu\text{m}$) than the aerobic fibers ($\sim 6.2 \mu\text{m}$), consistent with faster relative shortening velocity of the glycolytic fibers (Perry et al., 2009). The glycolytic fibers are also significantly longer than the aerobic fibers, which

contributes to faster absolute shortening velocity (Perry et al., 2009). Overall, the mid-region glycolytic fibers seem to be specialized for brief explosive sprints, while the more aerobic fibers appear to sustain slower walking gaits (Perry et al., 2009). This division of labor is in step with the roles of glycolytic and aerobic fibers that power swimming in portunid crabs, where activation of the glycolytic fibers is reserved for bursts of fast swimming and prolonged swimming is powered by the aerobic fibers (Hoyle and Burrows, 1973).

The general anatomical organization of the glycolytic and aerobic fiber types in ghost crabs is consistent with broad patterns observed in crustacean muscles (Medler and Mykles, 2015). Glycolytic fibers are larger in diameter across all size classes, but aerobic fibers become progressively more subdivided by membrane invaginations as muscles grow larger (Figs 2 and 3) (Hardy et al., 2009; Johnson et al., 2004). Hypertrophic growth of crustacean glycolytic fibers may favor energetic efficiency (Jimenez et al., 2011, 2013), but the large diameters significantly limit their diffusive capacity (Hardy et al., 2009, 2010, 2006; Kinsey et al., 2007). Membrane clefts subdividing aerobic fibers are lined with mitochondria and this arrangement fuels aerobic muscle contraction. The effective diameter of the aerobic fiber subdivisions reaches an asymptote at approximately 75–80 μm in ghost crabs (Figs 2 and 3).

The skeletal muscles of other highly active decapods exhibit similar adaptations for aerobic power output. Blue crabs, and other related swimming species of the family Portunidae, possess highly aerobic muscles that power specialized swimming appendages (Hartnoll, 1971). In these portunid crabs, the fifth pereopods have evolved into paddles that support prolonged swimming at speeds of up to 0.8 m s^{-1} (Spirito, 1972). The muscles that power swimming have been studied in some detail and comprise both aerobic and glycolytic fiber regions (Hoyle, 1973; Hoyle and Burrows, 1973; Tse et al., 1983; White and Spirito, 1973). The aerobic fibers display extensive subdivisions lined with high densities of mitochondria that comprise ~ 25 – 50% of the muscle cell volume (Hardy et al., 2009; Hoyle, 1973; Johnson et al., 2004; Tse et al., 1983). These mitochondrial densities put the portunid crab swimming muscles on par with highly aerobic vertebrate muscles (Moon and Tullis, 2006).

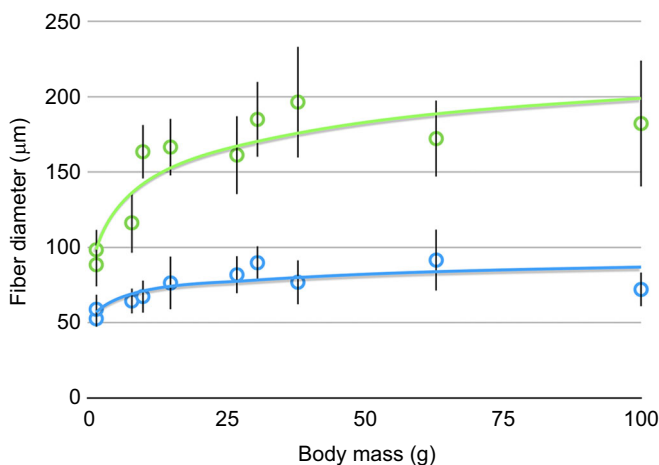


Fig. 3. Fiber diameters as a function of body size ($n=10$ crabs) in *O. quadrata*. In each case, glycolytic fibers (green) were larger than aerobic (blue) fiber diameters. Twenty fibers were measured for each point on the graph (\pm s.d.). Both glycolytic and aerobic fibers were measured from crabs ranging in body mass from approximately 1.5 to 100 g. Both fiber types increased in diameter in larger crabs, but the aerobic fiber diameter approached an asymptote and remained level at approximately 75–80 μm . The stable diameters of these fibers appear to result from the subdivisions that develop with increasing body size, as shown in Fig. 2.

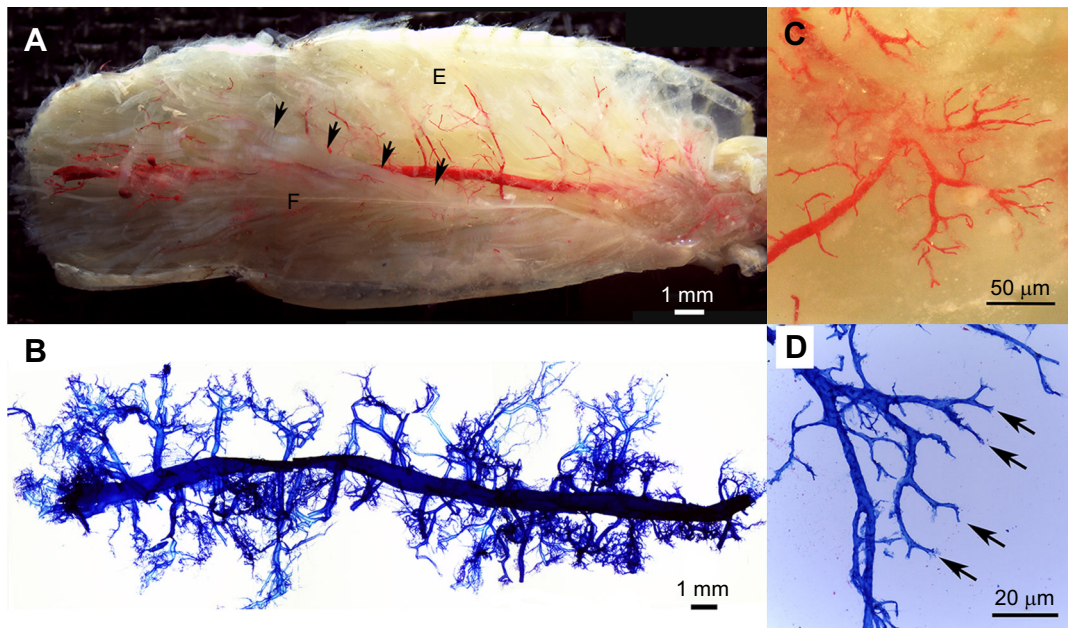


Fig. 4. Organization of the blood vessels supplying the muscles of the meropodite in *O. quadrata*. (A) Blood vessels were filled with Batson monomer and permitted to polymerize. The distal portion of the flexor muscle was removed (arrows indicate the remaining margin) to reveal the blood vessels. The main artery courses between the extensor (E) and flexor (F) muscles and supplies secondary vessels that supply both muscles at regular intervals. (B) Unfilled blood vessel removed from another crab and stained with Methylene Blue. Secondary branches subdivide into smaller and smaller vessels that ultimately form capillary-like structures. (C,D) Terminal capillary-like vessels supply muscle fibers. (C) Batson polymer filled vessels *in situ* with surrounding muscle tissue. (D) Methylene Blue-stained vessels in isolated artery. The width of the capillary-like vessels (arrows) is approximately 1–2 μm .

Both fiber types in blue crabs possess a high level of glycolytic potential, but aerobic fibers possess ~ 5 times greater citrate synthase activity and ~ 20 times greater sarcolemmal carbonic anhydrase activity than the glycolytic fibers (Henry et al., 2001). In vertebrates, maximum aerobic capacity is determined in large part by the aerobic potential of skeletal muscles (Weibel and Hoppeler, 2005), so it makes sense that the outstanding swimming abilities of these crabs is supported by their highly aerobic muscle fibers.

Aerobic exercise capacity in swimming crabs and running ghost crabs is clearly sustained by similar adaptations of their skeletal muscles. The aerobic muscles in both animals are devoid of membrane invaginations in the smallest crabs, but these fibers become increasingly subdivided as the crabs grow larger (Figs 2 and 3) (Hardy et al., 2009; Johnson et al., 2004). However, it appears that the degree of fiber subdivision is less extensive in the ghost crab. For example, our results show that the subdivision diameters in ghost crabs approach an asymptote at approximately 75–80 μm (Fig. 3), whereas the average subdivision diameter for all size classes of blue crabs averages approximately 35 μm (Johnson et al., 2004). This difference suggests that the swimming muscles are more specialized for sustained aerobic power output. The muscles that power prolonged swimming are highly specialized for sustained activity and exhibit stereotyped motor patterns driven by an isolated oscillator circuit (Spirito, 1972). Ghost crabs moving freely in their natural environment typically move intermittently, with rest periods occupying between 66% and 75% of their total activity (Weinstein, 1995, 2001). Sprinting at or above the maximal sustained aerobic speed only accounts for between 2.4% and 16.1% of their movements (Weinstein, 1995). Intermittent activity, followed by periods of recovery, may be used to extend the overall duration and total distance of activity during nightly foraging (Weinstein, 1995, 2001). The aerobic fibers may facilitate metabolic recovery of the more glycolytic fibers following bouts of exercise, as has been

proposed for blue crab muscles (Johnson et al., 2004). Another potentially important difference between these animals is that swimming crabs breathe water, whereas ghost crabs breathe air.

Decapod crustaceans possess a well-developed vascular system that has been described as being ‘partially closed’ because hemolymph is distributed through well-developed arteries that ramify into tissues to supply them with O_2 and nutrients (McGaw, 2005; Reiber and McGaw, 2009). The heart is constructed of striated muscle fibers and dynamic cardiac output is regulated by neural and hormonal control. The sternal artery is one of seven major arteries leaving the heart and receives most of the hemolymph (40–85%) ejected from the heart (McGaw and Reiber, 2015). This artery then divides to supply hemolymph to the legs and sends off regular branches into the surrounding muscles (Fig. 4A,B). These branches eventually lead into capillary-like vessels (Fig. 4C,D) that empty into lacunae, where hemolymph perfuses the tissues directly (Hill et al., 2016; McGaw and Reiber, 2015; McMahan and Burggren, 1988; Reiber and McGaw, 2009). Lang et al. (1972) reported that extensive ramifications of blood vessels in crayfish skeletal muscles closely follow motor nerves. The terminal ends of the capillary-like vessels apparently merge with the sarcolemma (Lang et al., 1972). Metabolically active tissues in decapod crustaceans reportedly possess especially high densities of these capillary-like vessels (McGaw and Reiber, 2015; McMahan and Burggren, 1988).

Crustacean capillary-like vessels ultimately empty their hemolymph into lacunae, which are irregular spaces formed between the muscle tissues and the integument lining the exoskeleton (Göpel and Wirkner, 2020; Greenaway and Farrelly, 1984; McGaw, 2005; McGaw and Reiber, 2015; McMahan and Burggren, 1988). Because these spaces are not completely lined with an endothelial layer of cells, the hemolymph bathes the muscle tissues directly (Göpel and Wirkner, 2020; Greenaway and Farrelly, 1984; McGaw, 2005; McMahan and Burggren, 1988).

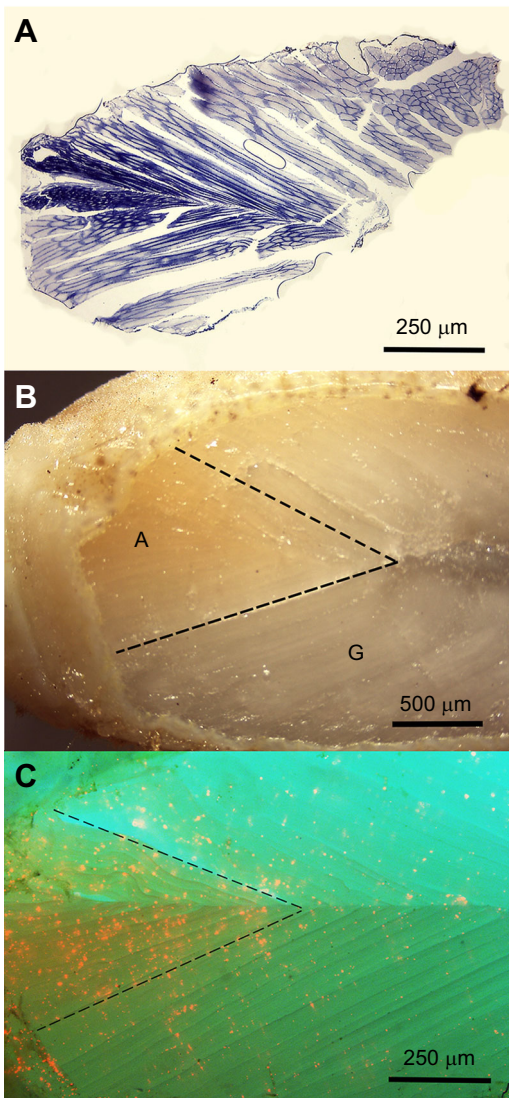


Fig. 5. Correspondence between aerobic/glycolytic fiber types and hemolymph flow as determined by fluorescent microspheres.

(A) Extensor muscle section stained with NADH-tetrazolium reductase to identify aerobic fibers. Intensely stained fibers are located in the proximal muscle region and appear as a wedge where the fibers insert onto the apodeme. (B) Extensor muscle demonstrating dark colored muscle in fresh tissue. The exoskeleton and integument have been removed to reveal the muscle tissue. Aerobic fibers in the proximal extensor (A) are brownish in color compared with the white glycolytic muscle (G). (C) Overlaid images of fluorescent microspheres and white light illuminated extensor muscle from a crab injected with microspheres. Microspheres appear to be concentrated within the proximal aerobic region of the muscle. Dashed lines in B and C indicate the approximate border between the aerobic and glycolytic fibers.

These lacunae connect with larger leg sinuses to transmit hemolymph into the infrabranchial sinus, which subsequently supplies hemolymph to the gills. After flowing through the gills, the hemolymph collects within the pericardial sinus and is returned to the heart. The returned hemolymph enters back into the heart chamber through several ostia (McGaw, 2005; McGaw and Reiber, 2015; McMahan and Burggren, 1988). Our observations of fluorescent particles moving in streams along the margins of the meropodite are consistent with the idea that the lacunae and sinuses form well defined conduits for hemolymph flow (McGaw, 2005; McGaw and Reiber, 2015).

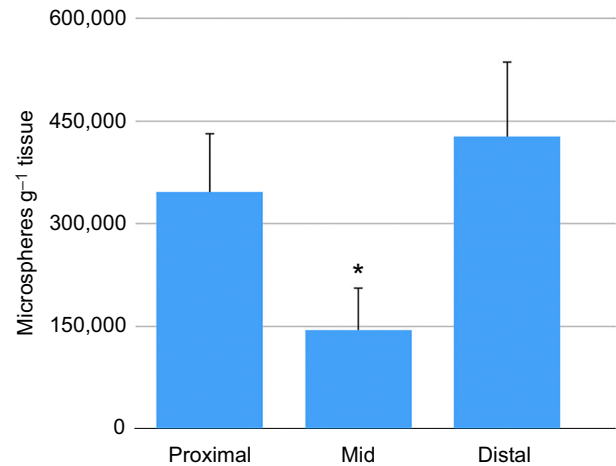


Fig. 6. Average number of microspheres per gram of muscle tissue from proximal, mid-region and distal parts of *O. quadrata* crab leg muscles ($n=5$). The number of microspheres was significantly lower in the glycolytic mid-region of the leg muscles compared with the more aerobic proximal and distal muscle regions as determined by a Tukey's *post hoc* ANOVA test ($*P<0.0001$). Data are means+s.d.; total number of injected microspheres was 3.6×10^7 .

Whether the more aerobic fibers in ghost crabs are supplied by a greater number of capillary-like vessels than glycolytic fibers within the same muscles is still unclear. Comparative studies of capillary supply to vertebrate skeletal muscles have documented important evolutionary trends in aerobic muscles (Mathieu-Costello, 1993; Weibel and Hoppeler, 2005). Maximum metabolic rate is strongly correlated with total mitochondrial volume of skeletal muscles, which are supplied with O_2 by a proportional density of capillaries (Weibel and Hoppeler, 2005). The principal adaptation that ensures adequate capillary density is a significant reduction in muscle fiber diameter, whereas the number of capillaries surrounding a fiber is only modestly increased (Mathieu-Costello, 1993). Effective fiber size of aerobic crab muscles is similarly maintained within lower limits through continual subdivision by membrane clefts, but information about the density of capillary-like vessels is limited. The study by Govind and Guchardi (1986) provides evidence for a similar number of capillary-like vessels per fiber (six to seven) in lobster muscles compared with vertebrates, but they did not find fiber type differences in capillary number. Electron microscopic data of blue crab muscles demonstrated the presence of capillaries within the subdivisions of aerobic fibers, but capillary densities were not reported (Johnson et al., 2004). The arterial branching patterns documented in the present study do not reveal dramatic differences among different regions (proximal, mid-region or distal) of the vessels, although the mid-region of the vessels seem to possess a slightly lower density of branches (Fig. 4B). Furthermore, the blood vessels in ghost crab legs exhibit extensive branching to supply muscles, but these vessels appear to be fairly unremarkable when compared with those of other decapod crustaceans, which also exhibit dramatic branching patterns (McGaw and Reiber, 2015).

Another possibility for the selective delivery of hemolymph to metabolically active aerobic fibers is through physiological regulation of hemolymph flow. In vertebrates, smooth muscles within the arterioles function as pre-capillary sphincters to dynamically regulate blood flow into metabolically active tissues (Hill et al., 2016). Although crustacean arteries are generally devoid of muscle fibers, they nevertheless possess mechanisms to selectively distribute

hemolymph to more metabolically active tissues, including myogenic control of valves at the entry points to major arteries (McGaw and Reiber, 2015; McMahon, 2001; Wilkens, 1997). Wilkens et al. (2008) also reported contractility of all major blood vessels in the lobster in response to application of glutamate and proctolin. Although myofibrils could not be identified, biochemical analyses of the vessels demonstrated the presence of myofibrillar proteins typical of skeletal muscles (Wilkens et al., 2008). Additionally, ultrastructural studies revealed dense bands of actin filaments, surrounded by microtubules, that could represent a mechanism for changes in vessel diameter (Cavey et al., 2008; Chan et al., 2006). The mechanisms that alter vessel resistance and control regional hemolymph flow in crustaceans remain obscure, but there is good evidence that the arteries are not the simple capacitance vessels they were once thought to be.

The present study confirms and extends our understanding of the linkages between the cardiovascular system and skeletal muscle organization in decapod crustaceans. The aerobic fibers of highly active crustaceans are replete with mitochondrial-line clefts that effectively subdivide the muscle to overcome limitations of diffusion. The cardiovascular system of ghost crabs is well developed to supply these active muscle fibers with the O₂ and nutrients that fuel contraction. Moreover, hemolymph flow into the muscle regions with aerobic fibers is significantly greater than that supplying the glycolytic fiber locations. It is unclear whether this selective hemolymph supply stems from physiological regulation of hemolymph flow, or from a greater density of vessel branches (Fig. 4). Our understanding of capillary supply, myogenic regulation of hemolymph flow, and skeletal muscle organization in crustaceans remains rudimentary. Future studies are needed to better understand the control of hemolymph flow into metabolically active regions of skeletal muscles in active crustaceans.

Acknowledgements

This study was completed in partial fulfillment of a Master's degree (S.Y.) at SUNY Fredonia. The research was generously supported by summer research fellowships from the Holmberg Foundation to S.Y., T.D.D. and R.R. An earlier version of this work was presented at the 2017 Annual Meeting of the Society for Integrative and Comparative Biology (Douglas et al., 2017).

Competing interests

The authors declare no competing or financial interests.

Author contributions

Conceptualization: S.M.; Methodology: T.D.D., S.M.; Formal analysis: S.Y., R.R., S.M.; Investigation: S.Y., R.R., T.D.D., S.M.; Data curation: S.Y., R.R., T.D.D., S.M.; Writing - original draft: S.M.; Writing - review & editing: S.Y., R.R., T.D.D.

Funding

This research received funding from the Holmberg Foundation.

References

- Brodal, P., Ingjer, F. and Hermansen, L.** (1977). Capillary supply of skeletal muscle fibers in untrained and endurance-trained men. *Am. J. Physiol.* **232**, H705-H712. doi:10.1152/ajpheart.1977.232.6.H705
- Burrows, M. and Hoyle, G.** (1973). The mechanism of rapid running in the ghost crab, *Ocypode ceratophthalma*. *J. Exp. Biol.* **58**, 327-349. doi:10.1242/jeb.58.2.327
- Cavey, M. J., Chan, K. S. and Wilkens, J. L.** (2008). Microscopic anatomy of the thin-walled vessels leaving the heart of the lobster *Homarus americanus*: anterior median artery. *Invertebr. Biol.* **127**, 189-200. doi:10.1111/j.1744-7410.2007.00124.x
- Chan, K. S., Cavey, M. J. and Wilkens, J. L.** (2006). Microscopic anatomy of the thin-walled vessels leaving the heart of the lobster *Homarus americanus*: anterior lateral arteries. *Invertebr. Biol.* **125**, 70-82. doi:10.1111/j.1744-7410.2006.00042.x
- Douglas, T., Abrantes, A. A. and Medler, S.** (2017). Arterial blood supply to skeletal muscles in ghost crabs. *Integr. Comp. Biol.* **57**, E42.
- Dubowitz, V. and Sewry, C. A.** (2007). *Muscle Biopsy. A Practical Approach*. Elsevier.
- Full, R. J. and Herreid, C. F.** (1983). Aerobic response to exercise of the fastest land crab. *Am. J. Physiol.* **244**, R530-R536. doi:10.1152/ajpregu.1983.244.4.R530
- Gerry, S. P. and Ellerby, D. J.** (2014). Resolving shifting patterns of muscle energy use in swimming fish. *PLoS ONE* **9**, e106030. doi:10.1371/journal.pone.0106030
- Glaser, B., You, G., Zhang, M. and Medler, S.** (2010). Relative proportions of hybrid fibers are unaffected by 6 weeks of running exercise in mouse skeletal muscles. *Exp. Physiol.* **95**, 211-221. doi:10.1113/expphysiol.2009.049023
- Göpel, T. and Wirkner, C.** (2020). The circulatory system of *Penaeus vannamei* Boone, 1931—Lacunar function and a reconsideration of the 'open vs. closed system' debate. *J. Morphol.* **281**, 500-512. doi:10.1002/jmor.21117
- Govind, C. K. and Guchardi, J.** (1986). Vascularization of a lobster muscle. *J. Morphol.* **188**, 327-333. doi:10.1002/jmor.1051880307
- Greenaway, P. and Farrelly, C. A.** (1984). The venous system of the terrestrial crab *Ocypode cordimanus* (Desmarest 1825) with particular reference to the vasculature of the lungs. *J. Morphol.* **181**, 133-142. doi:10.1002/jmor.1051810202
- Hafemann, D. R. and Hubbard, J. I.** (1969). On the rapid running of ghost crabs (*Ocypode ceratophthalma*). *J. Exp. Zool.* **170**, 25-32. doi:10.1002/jez.1401700103
- Hardy, K. M., Locke, B., Da Silva, M. and Kinsey, S.** (2006). A reaction-diffusion analysis of energetics in large muscle fibers secondarily evolved for aerobic locomotor function. *J. Exp. Biol.* **209**, 3610-3620. doi:10.1242/jeb.02394
- Hardy, K. M., Dillaman, R. M., Locke, B. R. and Kinsey, S. T.** (2009). A skeletal muscle model of extreme hypertrophic growth reveals the influence of diffusion on cellular design. *Am. J. Physiol. Regul. Integr. Comp. Physiol.* **296**, R1855-R1867. doi:10.1152/ajpregu.00076.2009
- Hardy, K. M., Lema, S. C. and Kinsey, S. T.** (2010). The metabolic demands of swimming behavior influence the evolution of skeletal muscle fiber design in the brachyuran crab family Portunidae. *Mar. Biol.* **157**, 221-236. doi:10.1007/s00227-009-1301-3
- Hartnoll, R. G.** (1971). The occurrence, methods, and significance of swimming in the Brachyura. *Anim. Behav.* **19**, 34-50. doi:10.1016/S0003-3472(71)80132-X
- Henry, R. P., Bilger, S. M. and Moss, A. G.** (2001). Carbonic anhydrase isozyme distribution and characterization in metabolic fiber types of the dorsal levator muscle of the blue crab, *Callinectes sapidus*. *J. Exp. Zool.* **290**, 234-246. doi:10.1002/jez.1054
- Herreid, C. F. and Full, R. J.** (1988). Energetics and Locomotion. In *Biology of Land Crabs* (ed. W. W. Burggren and B. R. McMahon), pp. 333-337. Cambridge: Cambridge University Press.
- Hill, R. W., Wyse, G. A. and Anderson, M.** (2016). *Animal Physiology*. Sunderland, MA: Sinauer Associates, Inc.
- Hoyle, G.** (1973). Correlated physiological and ultrastructural studies on specialized muscles. IIb. Fine-structure of power-stroke muscle of swimming leg of *Portunus sanguinolentus*. *J. Exp. Zool.* **185**, 97-109. doi:10.1002/jez.1401850110
- Hoyle, G.** (1983). *Muscles and their Neural Control*. New York: Wiley Interscience.
- Hoyle, G. and Burrows, M.** (1973). Correlated physiological and ultrastructural studies on specialized muscles. IIIa. neuromuscular physiology of power-stroke muscle of swimming leg of *Portunus sanguinolentus*. *J. Exp. Zool.* **185**, 83-95. doi:10.1002/jez.1401850109
- Jimenez, A., Dasika, S., Locke, B. and Kinsey, S.** (2011). An evaluation of muscle maintenance costs during fiber hypertrophy in the lobster *Homarus americanus*: are larger muscle fibers cheaper to maintain? *J. Exp. Biol.* **214**, 3688-3697. doi:10.1242/jeb.060301
- Jimenez, A., Dillaman, R. M. and Kinsey, S. T.** (2013). Large fibre size in skeletal muscle is metabolically advantageous. *Nat. Commun.* **4**, 2150. doi:10.1038/ncomms3150
- Johnson, L. K., Dillaman, R. M., Gay, D. M., Blum, J. E. and Kinsey, S. T.** (2004). Metabolic influences of fiber size in aerobic and anaerobic locomotor muscles of the blue crab, *Callinectes sapidus*. *J. Exp. Biol.* **207**, 4045-4056. doi:10.1242/jeb.01224
- Kinsey, S. T., Hardy, K. M. and Locke, B. R.** (2007). The long and winding road: influences of intracellular metabolite diffusion on cellular organization and metabolism in skeletal muscle. *J. Exp. Biol.* **210**, 3505-3512. doi:10.1242/jeb.000331
- Lang, F., Atwood, H. L. and Morin, W. A.** (1972). Innervation and vascular supply of the crayfish opener muscle: scanning and transmission electron microscopy. *Z. Zellforsch.* **127**, 189-200. doi:10.1007/BF00306801
- Marsh, R. L. and Ellerby, D. J.** (2006). Partitioning locomotor energy use among and within muscles: muscle blood flow as a measure of muscle oxygen consumption. *J. Exp. Biol.* **209**, 2385-2394. doi:10.1242/jeb.02287
- Marsh, R. L., Ellerby, D. J., Carr, J. A., Henry, H. T. and Buchanan, C. I.** (2004). Partitioning the energetics of walking and running: swinging the limbs is expensive. *Science* **303**, 80-83. doi:10.1126/science.1090704
- Mathieu-Costello, O.** (1993). Comparative aspects of muscle capillary supply. *Annu. Rev. Physiol.* **55**, 505-525. doi:10.1146/annurev.ph.55.030193.002443
- McGaw, I. J.** (2005). The decapod crustacean circulatory system: a case that is neither open nor closed. *Microsc. Microanal.* **11**, 18-36. doi:10.1017/S1431927605050026
- McGaw, I. J. and Reiber, C. L.** (2002). Cardiovascular system of the blue crab *Callinectes sapidus*. *J. Morphol.* **251**, 1-21. doi:10.1002/jmor.1071
- McGaw, I. J. and Reiber, C. L.** (2015). Circulatory physiology. In *The Natural History of the Crustacea*, Vol. IV, (ed. E. S. Chang and M. Thiel), pp. 199-246. Oxford University Press.

- McMahon, B. R.** (2001). Control of cardiovascular and its evolution in Crustacea. *J. Exp. Biol.* **204**, 923-932. doi:10.1242/jeb.204.5.923
- McMahon, B. R. and Burggren, W. W.** (1988). Circulation. In *Biology of the Land Crabs* (ed. W. W. Burggren and B. R. McMahon), pp. 298-332. Cambridge: Cambridge University Press.
- Medler, S. and Mykles, D. L.** (2015). Muscle structure, fiber types, and physiology. In *The Natural History of the Crustacea*, Vol. IV, (ed. E. S. Chang and M. Thiel), pp. 103-133. Oxford University Press.
- Moon, B. R. and Tullis, A.** (2006). The ontogeny of contractile performance and metabolic capacity in a high frequency muscle. *Physiol. Biochem. Zool.* **79**, 20-30. doi:10.1086/498195
- Neter, J., Wasserman, W. and Kutner, M. H.** (1990). *Applied Linear Statistical Models: Regression, Analysis of Variance, and Experimental Designs*. Boston: Irwin.
- Paul, R. J., Bihlmayer, S., Comorgen, M. and Zhler, S.** (1994). The open circulatory system of spiders (*Eurypelma californicum*, *Pholcus phalangioides*): a survey of functional morphology and physiology. *Physiol. Zool.* **67**, 1360-1382. doi:10.1086/physzool.67.6.30163902
- Perry, M. J., Tait, J., Hu, J., White, S. C. and Medler, S.** (2009). Skeletal muscle fiber types in the ghost crab, *Ocypode quadrata*: implications for running performance. *J. Exp. Biol.* **212**, 673-683. doi:10.1242/jeb.023481
- Reiber, C. L. and McGaw, I. J.** (2009). A review of the 'open' and 'closed' circulatory systems: new terminology for complex invertebrate circulatory systems in light of current findings. *Int. J. Zool.* **2009**, 1-8. doi:10.1155/2009/301284
- Saltin, B. and Gollnick, P. D.** (1983). Skeletal muscle adaptability: significance for metabolism and performance. In *Handbook of Physiology* (ed. L. D. Peachey, R. H. Adrian and S. R. Geiger), pp. 555-631. Bethesda, MD: American Physiological Society.
- Spirito, C. P.** (1972). An analysis of swimming behavior in the portunid crab, *Callinectes sapidus*. *Mar. Behav. Physiol.* **1**, 261-276. doi:10.1080/10236247209386902
- Tse, F. W., Govind, C. K. and Atwood, H. L.** (1983). Diverse fiber composition of swimming muscles in the blue crab, *Callinectes sapidus*. *Can. J. Zool.* **61**, 52-59. doi:10.1139/z83-005
- Waters, R. E., Rotevatn, S., Li, P., Annex, B. H. and Yan, Z.** (2004). Voluntary running induces fiber type-specific angiogenesis in mouse skeletal muscle. *Am. J. Physiol. Cell Physiol.* **287**, C1342-C1348. doi:10.1152/ajpcell.00247.2004
- Weibel, E. R. and Hoppeler, H.** (2005). Exercise-induced maximal metabolic rate scales with muscle aerobic capacity. *J. Exp. Biol.* **208**, 1635-1644. doi:10.1242/jeb.01548
- Weinstein, R. B.** (1995). Locomotor behavior of nocturnal ghost crabs on the beach: focal animal sampling and instantaneous velocity from three-dimensional motion analysis. *J. Exp. Biol.* **198**, 989-999. doi:10.1242/jeb.198.4.989
- Weinstein, R. B.** (2001). Terrestrial intermittent exercise: common issues for human athletics and comparative animal locomotion. *Am. Zool.* **41**, 219-228. doi:10.1093/icb/41.2.219
- White, A. Q. and Spirito, C. P.** (1973). Anatomy and physiology of the swimming leg musculature in the blue crab, *Callinectes sapidus*. *Mar. Behav. Physiol.* **2**, 141-153. doi:10.1080/10236247309386921
- Whittemore, S. B., Hoglin, B., Green, M. and Medler, S.** (2015). Stride frequency in relation to allometric growth in ghost crabs (*Ocypode quadrata*). *J. Zool.* **296**, 286-294. doi:10.1111/jzo.12244
- Wilkens, J. L.** (1997). Possible mechanisms of control of vascular resistance in the lobster *Homarus americanus*. *J. Exp. Biol.* **200**, 487-493. doi:10.1242/jeb.200.3.487
- Wilkens, J. L., Cavey, M. J., Shovkivska, I., Zhang, M. L. and ter Keurs, H.** (2008). Elasticity, unexpected contractility and the identification of actin and myosin in lobster arteries. *J. Exp. Biol.* **211**, 766-772. doi:10.1242/jeb.007658
- Wong, L. E., Garland, T., Rowan, S. L. and Hepple, R. T.** (2009). Anatomic capillarization is elevated in the medial gastrocnemius muscle of mighty mini mice. *J. Appl. Physiol.* **106**, 1660-1667. doi:10.1152/jappphysiol.91233.2008